Eurographics Workshop on Visual Computing for Biology and Medicine (2020)
K. Nieselt and R. G. Raidou (Editors)

Short Paper

VirtualDSA++: Automated Segmentation, Vessel Labeling, Occlusion Detection and Graph Search on CT-Angiography Data

F. Thamm [1,2], M. Jürgens [2], H. Ditt [2] and A. Maier [1]

[1]Friedrich-Alexander-University Pattern Recognition Lab, Erlangen, Germany
[2]Siemens Healthcare GmbH, Forchheim, Germany

Abstract

Computed Tomography Angiography (CTA) is one of the most commonly used modalities in the diagnosis of cerebrovascular diseases like ischemic strokes. Usually, the anatomy of interest in ischemic stroke cases is the Circle of Willis and its peripherals, the cerebral arteries, as these vessels are the most prominent candidates for occlusions. The diagnosis of occlusions in these vessels remains challenging, not only because of the large amount of surrounding vessels but also due to the large number of anatomical variants. We propose a fully automated image processing and visualization pipeline, which provides a full segmentation and modelling of the cerebral arterial tree for CTA data. The model itself enables the interactive masking of unimportant vessel structures e.g. veins like the Sinus Sagittalis, and the interactive planning of shortest paths meant to be used to prepare further treatments like a mechanical thrombectomy. Additionally, the algorithm automatically labels the cerebral arteries (Middle Cerebral Artery left and right, Anterior Cerebral Artery short, Posterior Cerebral Artery left and right) detects occlusions or interruptions in these vessels. The proposed pipeline does not require a prior non-contrast CT scan and achieves a comparable segmentation appearance as in a Digital Subtraction Angiography (DSA).

CCS Concepts

• Computing methodologies → Image segmentation; Search with partial observations; • Human-centered computing → Visualization;

1. Introduction

Strokes in general are defined as an abrupt onset of a focal neurological deficit caused by a lack of blood supply. Either spontaneous ruptures (hemorrhagic type) or artery occlusions (ischemic type) can be causes of an undersupply of the cerebrovascular parenchyma [WS12]. Due to the speed, high availability and the ability to acquire highly resolved images CT became the most widely used modality for the diagnosis of acute strokes [SRKD07, LFR*01]. The diagnosis of ischemic strokes is usually been done using the Computed Tomography Angiography (CTA), in particular in order to localize intravascular thrombi that can be targeted for a thrombolysis and/or mechanical thrombectomy [tor13]. These thrombi result in so called (vessel) occlusions, which block the blood flow in arteries and cause an undersupply of blood in the respective parenchyma. Consequently as no contrast agent passes through the occlusion, the entire subtree is not contrast enhanced. The diagnosis of ischemic strokes remains challenging, since the region of interest, the Circle of Willis and its peripheral vessels, the cerebral arteries are surrounded by other vessels and bone structures. This situation is aggravated by the large amount of anatomical variants of the Circle of Willis including the cerebrovascular system [Iqb13]. To know the patients actual vessel tree structure simplifies the planning for the thrombectomy significantly. Therefore, physicians need to have a good overview of all vessels highlighted by the CTA acquisition. DSA, the subtraction of a registered CTA and NCCT volume, provides the best view on all vessels. Still, DSA requires in total two acquisitions and hence two radial exposures. Furthermore DSA visualizes both, veins and arteries which is sometimes not desired either especially if a large contrast bolus was injected, because usually the cerebral arteries are the reason for acute strokes and thus of interest in the actual diagnosis.

We propose a method called VirtualDSA++ which leads to a DSA-like segmentation solely based on a CTA scan with no use of any prior NCCT scan. We name our approach VirtualDSA++ as no non-contrast CT scan is required for the proposed pipeline and comparable image appearances are achievable as in a DSA, hence the phrase "Virtual". The "++" stands for the algorithmic extensions, such as the path finding or selective vein suppression.

2. Related Work

In the last few years, several works have been published addressing the segmentation of the cerebrovascular tree. Most of these publications were based on MRI angiography (TOF), ranging from classic image processing [MMNG15, MMNG17] to deep learning methods and achieved good and promising results [LRA*19, LWF*17,

DOI: 10.2312/vcbm.20201181

TEF*18, HMA*20, CDY*18]. However, a segmentation on MRI angiography data can not be fairly compared to CTA data, since no other non-vessel structures can seriously interfere the segmentation. In CTA the presence of bone structures highly overlaps with vessel tissue regarding their intensity values and that as a difference to MRI makes it difficult to segment [LFP*17, HF07]. Due to the speed and the high availability CT is still a commonly used modality in the stroke diagnosis, especially as it is used in clinical practice as a first line imaging tool to distinguish the ischemic and the hemorrhagic type. Segmentations using CTA only are quite rare as they often incorporate a prior NCCT and process the conjunct data into DSA-like images before finally segmenting them [MVv*05, HF07]. With the use of deep learning methods Nazir et al. proposed 2020 a patch-wise segmentation network similar to a ResNet consisting of Inception Modules [SLJ*15]. In a cross validation setup they have achieved a Dice score of 89.46 %. But as in all supervised deep learning methods, labeled data is essential, and especially for the cerebrovascular vessel tree extremely time consuming to produce. Nazir et al. reported the annotation by hand of one single CTA data set takes five to six hours each [NCS*20], making the development of large scale applications or the reproducability very difficult.

The labeling of the Circle of Willis is a well studied field at least for MRI data. Atlas based approaches are the most commonly used way of realising the vessel labeling, e.g. as it was done with TOF MRI data in [VdGJB*15, MMNG17] and with 4D-flow MRI data by Dunas et al. [DWA*16] with the corresponding follow up work [DWA*17]. In all approaches, the atlas map is being labeled with respect to the vessel sections and after a registration compared to a data set at hand. All three publications achieve sensitivities between 90% and 100%. As these works also cover the computation of the respective atlas maps, only data sets of healthy patients were used, which makes a clinical evaluation hard for ischemic stroke cases. Nonetheless, the methods by Dunas et al. [DWA*16, DWA*17] can detect vessels missing due to anatomical variants but as no cases with large vessel occlusion were part of their work, no predictions can be done on how their method will perform on stroke cases. Labeling on CTA data compared to MRI data leads to the same challenges as in the segmentation: Bone tissue can easily be confused with perfused vessels and thus disturb the labeling.

The automated detection of large vessel occlusions on CTA data is also a recent field of study. Amukotuwa et al. [ASDB19] for instance, proposed 2019 a method for the automated detection of areas affected by large vessel occlusions. They proposed an image processing pipeline, which processes the CTA data and compares the intensity values of the vessel structures in both hemisphere area by area. Occlusion (positive class) were detected with a sensitivity of 96,% and a specificity of 79 %. However, the occlusion itself is not actually located in their work, rather the affected region. As an alternative to an image processing based approach, a Deep Learning based detection of the affected region has been done as well by Sheth et al. [SLRB*19]. In their work they have used a chain of Inception Modules [SLJ*15] using shared weights for both hemispheres, which shows similarities to Amukotuwa et al.'s work. As ground truth, they have used CTP acquisitions to determine the affected region and achieved an AUC of 88 %.

3. Segmentation

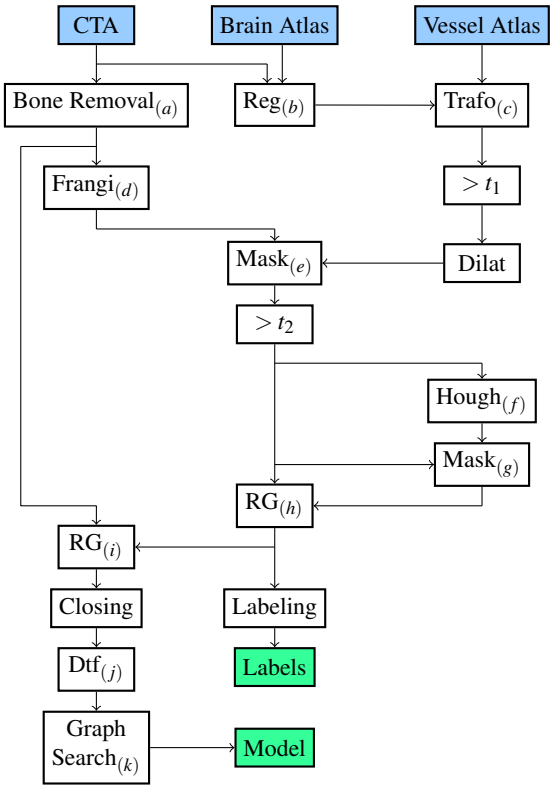

Figure 1: *Image processing pipeline for the segmentation, modelling and labeling of the cerebrovascular vessel tree. Inputs are marked as blue and outputs as green. Arrows which enter the boxes vertically represent images whereas arrows which enter horizontally are either masks or additional information required for the respective action, e.g. the transformation matrix resulting from (b) enters the trafo module (c) horizontally in order to transform the Vessel atlas.*

Figure 1 shows the image pipeline we propose, which leads automatically leads into the segmentation and subsequently into the modelling of the cerebrovascular vessel tree. In addition to that, the pipeline returns the label markers for the large cerebral vessels, Middle Cerebral Artery left and right (MCAL and MCAR), Anterior Cerebral Artery (ACA), Posterior Cerebral Artery left and right (PCAL and PCAR). The pipeline starts with the CTA data set where all bone structures are being segmented in (a) using the bone removal method by Chen et al. published in [CSKK*]. In parallel the CTA volume is being registered (b) onto the brain atlas by Kemmling et al. [KWB*12]. Both volumes are registered with a non-rigid transformation field using the in-house registration engine. The registration algorithm is a multi-scale dense matching method enabled by the gradient of the local cross correlation similarity measure. The deformations are estimated based on the composition of the time-dependent velocity fields combined with a Gaussien smoothing regularization. Alternatively, the volumes can be registered using publicly available registration tools as well. The resulting transformation field of (b) is reused to transform an at-

las again by Kemmling [FSF*12] specifically designed to represent the Circle of Willis and large vessels attached to it. The registered vessel atlas is binarized by thresholding ($t_1 = 0.005$) and dilated ($7 \times 7 \times 11$) to close noisy gaps that emerged by interpolations in the transformation. The result of (a) is filtered in (d) using the hessian based vesselness filter by Frangi et al (two scales, $\sigma_1 = 1.00$, $\sigma_u = 1.50$). [FNVV98] which reacts well on tubular structures as they occur on vessel shaped tissue. As vessel structures are not the only tissue where tubular structures might appear, the filter response is being masked out in (e) using the dilated vessel atlas described earlier. This removes large noisy clusters which typically appear in the nose region. The mask is further binarized using a threshold ($t_2 = 4$). In (f) a slice-wise Hough transformation on circles is applied on the thresholding result, to model the tubular structures enhanced by the vesselness filter. In (g) the circle centerpoints found in (f) are masked out using the binarized mask so only centerpoints are left which are inside of a vessel. The masked centerpoints of (g) are used as seed points for a region growing step in (h) using a relative threshold of 5%. Additionally, in order to remove noisy clusters, only connected components are returned with a volume larger than 10 ml. The result of (h) is forwarded into the labeling algorithm, described in Section 4, which yields the final label markers and moreover detects missing or occluded vessels. The resulting mask of (h), sampled as seed points is again used for a region growing step in (i), segmenting the boneless CTA scan from (a). Empirically an HU range between 130 HU and 1500 HU for the region growing led to the best and robust results. In order to fill tiny gaps, which occur in the broad vessel structures near the cerebellum, a slice-wise closing ($1 \times 1 \times 0$) is applied on (i) and modelled in (j) using the MeVisLab implementation of the Dtf-Skeletonization algorithm published by Selle [Sel00]. Finally, the graph algorithms described in Section 5, vein suppression and the path finding are applied in (k), representing the last step of the pipeline and return therefore the output model.

4. Vessel Labeling

The segmentation pipeline uses two different atlases. One for the brain tissue and one for the cerebrovascular structures. The labeling method we propose is enabled by placing multiple markers on the vessel atlas for each large vessel. After a registration of the brain atlas, these vessel markers are transformed into the CTA data set at hand. Figure 3 shows the markers placed on the Anterior Cerebral Artery and how they approximate the vessel pathway. To finally place a label to the corresponding vessels, our approach determines the closest point on the vessel segmentation wall to each marker and chooses the one with the smallest distance as the final marker. Either the marker itself or the closest point on the vessel can be used as label position. We extend the labeling concept by the proposal of a method to use the multiple markers as indicators for occluded vessels. For this matter our approach computes the distances of each marker to closest vessel wall. Firstly, if the distance from all markers to the next vessel is beyond the repsective radius, these markers are considered as missing. If 70 % of the multiple markers are classified as missing, the whole vessel is classified as occluded. All markers have individual radii dependent on the branch, defining the range within a vessel must be. The radii were determined empirically for the MC and ACA with 15 mm and for PCA with

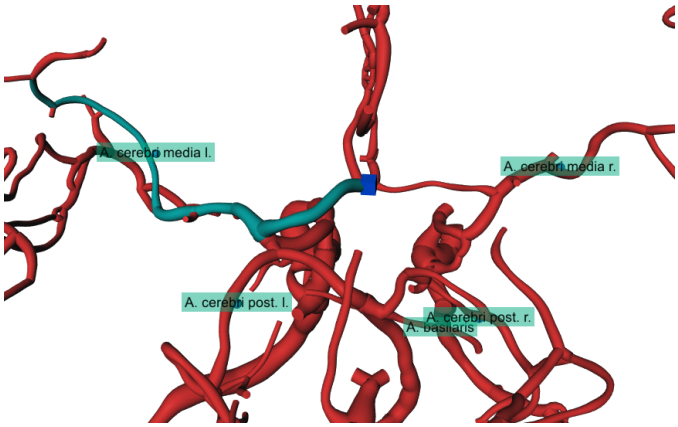

Figure 2: *VirtualDSA++ segmentation viewed on the Circle of Willis together with the internal placed label marker according to [VBR]. Highlighted in green is a path computed by the path search algorithm. The blue cube represents the root node, described later in Section 5.1*

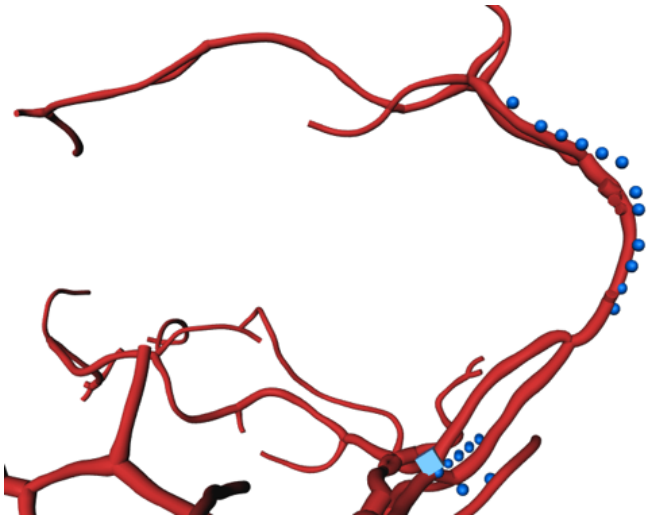

Figure 3: *VirtualDSA++ result together with the transformed marker chain on the top right approximating the ACA pathway. The marker displacements result from the coarse representation of probablistic vessel atlas.*

5 mm. If an occlusion is located closely next to the markers and the vessel model interrupts, all markers have a common closest point on the vessel wall. This leads to a linear increase of the distance measure with ascending marker index as the indexing goes in order from proximal to distal. A linear regression allows to compute the slope of the linear relation. Subsequently, the slope itself serves as an indicator for the occlusion. If the slope is small, the marker chain is placed rather parallel to the vessel. If the slope is large and positive, the marker chain diverges from the closest vessel point, thus an interruption in the vessel flow is to be expected. If the slope is negative, the marker chain approaches the vessel wall with ascending index, which can be caused by inaccuracies in the atlas and are not considered as an indicator for abnormalities.

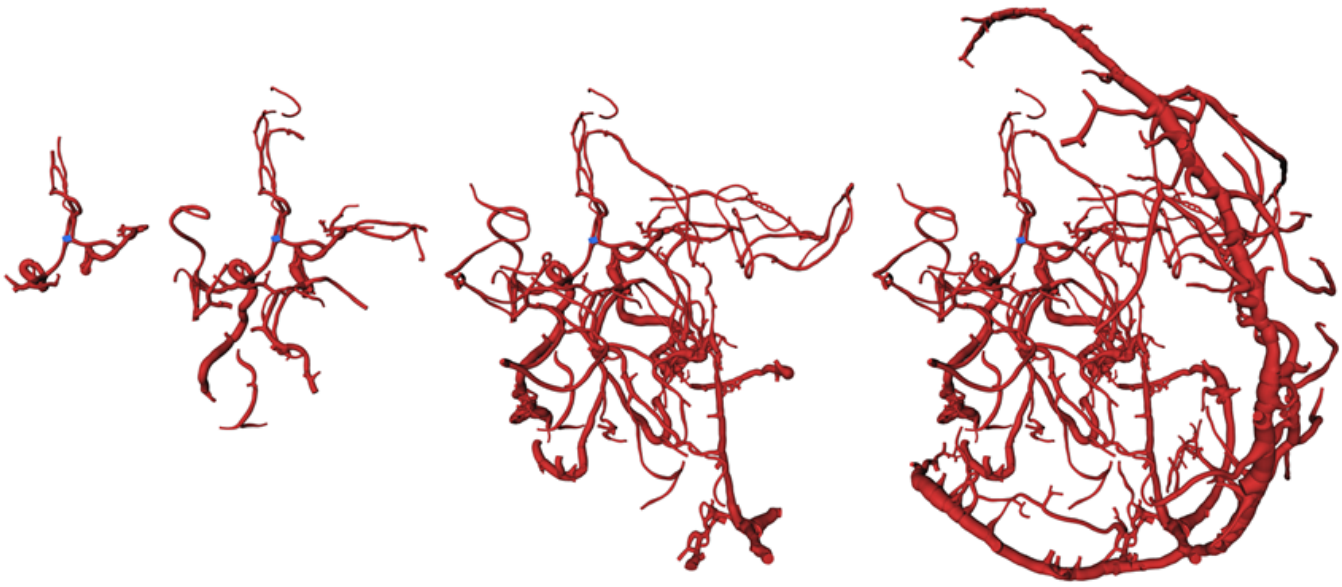

Figure 4: *Vein suppression feature of VirtualDSA++ on different distances. From left to right: 50 mm, 100 mm, 200 mm and 400 mm. The tiny blue cube is located at the Communicans Anterior Vessel and indicates the root node. Starting with 50 mm only vessels directly connected to the root node are rendered. Increasing the distance up to 400 mm reveals step by step all vessels found including parts not of interest in the ischemic stroke diagnosis, e.g. Sinus Sagittalis.*

5. Search on Models

Step (k) in Figure 1, described as "Graph Search" uses the vessel tree model computed in (j) as an algorithmic interface. First we introduce in Section 5.1 the path finding problem on the vessel model as a generic concept from which applications can be derived. Secondly we use the shortest distance as optimization problem and present two applications namely the path search in 5.2 and the interactive vein suppression in 5.3.

5.1. Iterative Search

The model in step (j) of the pipeline in Figure 1 can now be used to apply path search algorithms and with that applications arise. The search is based on bifurcation level instead of on pixel basis, as only bifurcations are relevant for any path decisions, which accelerates the algorithm significantly and allows an interactive use of it. The model of (j) itself is equivalent to a graph where all bifurcations represent nodes and vessel section represent edges. In an initial state, the user sets a so-called root node. The root node represents the node where for all nodes paths are computed to. The key idea is to apply the AI path search algorithm A* between the root node and all other nodes in the tree and cache internally all resulting paths to provide quick access. Based on the optimality criterion and heuristics chosen for the A* algorithm, different applications arise from that generic concept. In this publication, we take the computation of shortest distances to the root node as subject of optimization and present the features enabled by this. A* requires a heuristic, thus we choose the Euclidean distance between the current node and the root node. The real cost value is computed based on the actual length of a vessel section, not based on the distance between two nodes. Trees which are not attached to the root node can be rendered and be considered into the path search as well. Depending on the choice of the optimality criterion this is possible by determining the most optimal node in these unattached trees. These quasi-optimal nodes are treated again as root nodes within their own tree. For the shortest distance criterion the quasi-optimal node is the closest point of the unattached tree to the root node.

5.2. Path Search

The plain path search results can be used to be rendered as overlays to the model itself. Figure 2 shows the example for the path finding according the smallest distance rendered in green. This feature can be used to guide an interventional action or as an annotation tool for findings.

5.3. Vein Suppression

Vessel sections can be shown or concealed interactively according to their distance to the root node. For example, the ischemic stroke diagnosis becomes easier, if the root node is placed into the Circle of Willis, and the vein structures (Sinus Sagittalis) which are not of interest in the actual diagnosis are concealed, because they have large distances to the root node. In this case we call it vein suppression as veins are hidden in the first place. This is shown in Figure 4 for different walking distances ranging from 50 mm to 400 mm from Communicans Anterior Vessel as root node. Under this link, we provide additional video material for the demonstration of the interactive path finding and the vein suppression.

6. Conclusions

We proposed in this work an image processing pipeline, which segments automatically the cerebrovascular tree in CTA head scans,

and results in a modelling of the vessel system. In this publication, we presented the search for shortest pathways as the subject of optimization and derived two applications by that. Firstly, the rendering of shortest paths between two nodes, which might help interventions as a mechanical thrombectomy for instance. Secondly, we presented the interactive Vein Suppression as another feature derived from the path search on the tree model. This feature allows to interactively conceal parts of the vessel tree which are not of interest in the ischemic stroke diagnosis. Quantitative evaluations will follow in future works.

References

[ASDB19] AMUKOTUWA S. A., STRAKA M., DEHKHARGHANI S., BAMMER R.: Fast automatic detection of large vessel occlusions on ct angiography. *Stroke 50*, 12 (2019), 3431–3438. doi:10.1161/STROKEAHA.119.027076. 2

[CDY*18] CHEN H., DOU Q., YU L., QIN J., HENG P.-A.: Voxresnet: Deep voxelwise residual networks for brain segmentation from 3d mr images. *NeuroImage 170* (2018), 446–455. 1

[CSKK*] CHEN M., SOO KIM T., KRETSCHMER J., SEIFERT S., ZOUH S. K., SCHÖBINGER M., LIU D., XU Z., GRBIC S., ZHANG H.: Deep learning based bone removal in computed tomography angiography. 2

[DWA*16] DUNÅS T., WÅHLIN A., AMBARKI K., ZARRINKOOB L., BIRGANDER R., MALM J., EKLUND A.: Automatic labeling of cerebral arteries in magnetic resonance angiography. *Magma (New York, N.Y.) 29*, 1 (2016), 39–47. doi:10.1007/s10334-015-0512-5. 2

[DWA*17] DUNÅS T., WÅHLIN A., AMBARKI K., ZARRINKOOB L., MALM J., EKLUND A.: A stereotactic probabilistic atlas for the major cerebral arteries. *Neuroinformatics 15*, 1 (2017), 101–110. doi:10.1007/s12021-016-9320-y. 2

[FNVV98] FRANGI A. F., NIESSEN W. J., VINCKEN K. L., VIERGEVER M. A.: Multiscale vessel enhancement filtering. In *International conference on medical image computing and computer-assisted intervention* (1998), Springer, pp. 130–137. 3

[FSF*12] FORKERT N. D., SUNIAGA S., FIEHLER J., WERSCHING H., KNECHT S., KEMMLING A.: Generation of a probabilistic arterial cerebrovascular atlas derived from 700 time-of-flight mra datasets. In *MIE* (2012), pp. 148–152. 3

[HF07] HERNANDEZ M., FRANGI A. F.: Non-parametric geodesic active regions: method and evaluation for cerebral aneurysms segmentation in 3dra and cta. *Medical image analysis 11*, 3 (2007), 224–241. doi:10.1016/j.media.2007.01.002. 2

[HMA*20] HILBERT A., MADAI V. I., AKAY E. M., AYDIN O. U., BEHLAND J., SOBESKY J., GALINOVIC I., KHALIL A. A., TAHA A. A., WÜRFEL J., ET AL.: Brave-net: Fully automated arterial brain vessel segmentation in patients with cerebrovascular disease. *medRxiv* (2020). 1

[Iqb13] IQBAL S.: A comprehensive study of the anatomical variations of the circle of willis in adult human brains. *Journal of clinical and diagnostic research : JCDR 7*, 11 (2013), 2423–2427. doi:10.7860/JCDR/2013/6580.3563. 1

[KWB*12] KEMMLING A., WERSCHING H., BERGER K., KNECHT S., GRODEN C., NÖLTE I.: Decomposing the hounsfield unit: probabilistic segmentation of brain tissue in computed tomography. *Clinical neuroradiology 22*, 1 (2012), 79–91. doi:10.1007/s00062-011-0123-0. 2

[LFP*17] LELL M. M., FLEISCHMANN U., PIETSCH H., KORPORAAL J. G., HABERLAND U., MAHNKEN A. H., FLOHR T. G., UDER M., JOST G.: Relationship between low tube voltage (70 kv) and the iodine delivery rate (idr) in ct angiography: An experimental in-vivo study. *PloS one 12*, 3 (2017), e0173592. doi:10.1371/journal.pone.0173592. 2

[LFR*01] LEV M. H., FARKAS J., RODRIGUEZ V. R., SCHWAMM L. H., HUNTER G. J., PUTMAN C. M., RORDORF G. A., BUONANNO F. S., BUDZIK R., KOROSHETZ W. J., ET AL.: Ct angiography in the rapid triage of patients with hyperacute stroke to intraarterial thrombolysis: accuracy in the detection of large vessel thrombus. *Journal of computer assisted tomography 25*, 4 (2001), 520–528. 1

[LRA*19] LIVNE M., RIEGER J., AYDIN O. U., TAHA A. A., AKAY E. M., KOSSEN T., SOBESKY J., KELLEHER J. D., HILDEBRAND K., FREY D., MADAI V. I.: A u-net deep learning framework for high performance vessel segmentation in patients with cerebrovascular disease. *Frontiers in neuroscience 13* (2019), 97. doi:10.3389/fnins.2019.00097. 1

[LWF*17] LI W., WANG G., FIDON L., OURSELIN S., CARDOSO M. J., VERCAUTEREN T.: On the compactness, efficiency, and representation of 3d convolutional networks: Brain parcellation as a pretext task. *0302-9743 10265*, 9 (2017), 348–360. doi:10.1007/978-3-319-59050-9{\textunderscore}28. 1

[MMNG15] MIAO H., MISTELBAUER G., NASEL C., GRÖLLER M. E.: Cowradar: Visual quantification of the circle of willis in stroke patients. In *VCBM* (2015), pp. 1–10. 1

[MMNG17] MIAO H., MISTELBAUER G., NAŠEL C., GRÖLLER M. E.: Visual quantification of the circle of willis: An automated identification and standardized representation. In *Computer Graphics Forum* (2017), vol. 36, Wiley Online Library, pp. 393–404. 1, 2

[MVv*05] MANNIESING R., VELTHUIS B. K., VAN LEEUWEN M. S., VAN DER SCHAAF I. C., VAN LAAR P. J., NIESSEN W. J.: Level set based cerebral vasculature segmentation and diameter quantification in ct angiography. 2

[NCS*20] NAZIR A., CHEEMA M. N., SHENG B., LI H., LI P., YANG P., JUNG Y., QIN J., KIM J., FENG D. D.: Off-enet: An optimally fused fully end-to-end network for automatic dense volumetric 3d intracranial blood vessels segmentation. *IEEE Transactions on Image Processing* (2020), 1. doi:10.1109/TIP.2020.2999854. 2

[Sel00] SELLE D.: *Analyse von Gefäßstrukturen in medizinischen Schichtdatensätzen für die comutergestützte Operationsplanung*. PhD thesis, 2000. 3

[SLJ*15] SZEGEDY C., LIU W., JIA Y., SERMANET P., REED S., ANGUELOV D., ERHAN D., VANHOUCKE V., RABINOVICH A.: Going deeper with convolutions. In *Proceedings of the IEEE conference on computer vision and pattern recognition* (2015), pp. 1–9. 2

[SLRB*19] SHETH S. A., LOPEZ-RIVERA V., BARMAN A., GROTTA J. C., YOO A. J., LEE S., INAM M. E., SAVITZ S. I., GIANCARDO L.: Machine learning-enabled automated determination of acute ischemic core from computed tomography angiography. *Stroke 50*, 11 (2019), 3093–3100. doi:10.1161/STROKEAHA.119.026189. 2

[SRKD07] SCHELLINGER P. D., RICHTER G., KÖHRMANN M., DÖRFLER A.: Noninvasive angiography (magnetic resonance and computed tomography) in the diagnosis of ischemic cerebrovascular disease. *Cerebrovascular Diseases 24*, Suppl. 1 (2007), 16–23. 1

[TEF*18] TETTEH G., EFREMOV V., FORKERT N. D., SCHNEIDER M., KIRSCHKE J., WEBER B., ZIMMER C., PIRAUD M., MENZE B.: Deepvesselnet: Vessel segmentation, centerline prediction, and bifurcation detection in 3-d angiographic volumes. *arXiv preprint arXiv:1803.09340* (2018). 1

[tor13] *The Stroke Book*, 2 ed. Cambridge University Press, 2013. doi:10.1017/CBO9781139344296. 1

[VBR] VIOLA I., BÜHLER K., ROPINSKI T.: Survey of labeling techniques in medical visualizations. 3

[VdGJB*15] VAN DE GIESSEN M., JANSSEN J. P., BROUWER P. A., REIBER J. H., LELIEVELDT B. P., DIJKSTRA J.: Probabilistic atlas based labeling of the cerebral vessel tree. In *Medical Imaging 2015: Image Processing* (2015), vol. 9413, International Society for Optics and Photonics, p. 94130V. 2

[WS12] WITTENAUER R., SMITH L.: Background paper 6.6 ischaemic and haemorrhagic stroke. *Priority Medicines For Europe And The World" A Public Health Approach To Innovation* (2012). 1